PROFESSOR MARIA DE LIMA (Orcid ID : 0000-0002-8277-3458)

Article type : Research Article

New Thiophene-Acridine Compounds: Synthesis, Antileishmanial Activity, DNA Binding, Chemometric and Molecular Docking Studies

Vanessa de Lima Serafim[a,f]; Mayara Barbalho Félix[a,f]; Daiana Karla Frade Silva[a,f]; Klinger Antônio da Franca Rodrigues[a,f], Patrícia Néris Andrade[a,f]; Sinara Mônica Vitalino de Almeida[c]; Sanderssonilo de Albuquerque dos Santos[d]; Jamerson Ferreira de Oliveira[d]; Maria do Carmo Alves de Lima[d]; Francisco Jaime Bezerra Mendonça-Junior[b,f]; Marcus Tullius Scotti[f]; Márcia Rosa de Oliveira[a]; Ricardo Olímpio de Moura[b,e*].

[a]*Laboratório de Leishmanioses, Departamento de Biologia Molecular, CEP 58051-970, Universidade Federal da Paraíba, João Pessoa, PB, Brazil;*

[b]*Laboratório de Síntese e Vetorização de Moléculas, Universidade Estadual da Paraíba, Departamento de Ciências Biológicas, CEP 58070-450, João Pessoa, PB, Brazil;*

[c]*Laboratório de Imunopatologia Keizo Asami (LIKA) and Departamento de Bioquímica, Universidade Federal de Pernambuco, Recife 50670-901, PE, Brazil;*

[d]*Laboratório de Química e Inovação Terapêutica (LQIT) - Departamento de Antibióticos, Universidade Federal de Pernambuco, Recife 50670-901, PE, Brazil;*

[e]*Departamento de Ciências Farmacêuticas, Centro de Ciências Biológicas e da Saúde, Universidade Estadual da Paraíba - Bodocongó, CEP: 58429-600, Campina Grande, PB, Brazil;*

[f]*Programa de Pós-Graduação em Produtos Naturais e Sintéticos Bioativos. Universidade Federal da Paraíba, João Pessoa, Paraíba 58059-900, Brazil;*

To whom correspondence should be addressed: Maria do Carmo Alves de Lima

**Email: nenalima.mariadocarmo@gmail.com*

This article has been accepted for publication and undergone full peer review but has not been through the copyediting, typesetting, pagination and proofreading process, which may lead to differences between this version and the Version of Record. Please cite this article as doi: 10.1111/cbdd.13176

Phone number: +55 8121268347
Fax: +55 8121268346

Abstract

In the present study, we synthesized eight new compounds containing the 2-amino-cycloalkyl[*b*]thiophene and acridine moieties (**ACT_{01}** and **ACS_{01}-ACS_{07}**). None tested compounds presented human erythrocyte cytotoxicity. The new compounds presented antipromastigote activity, where **ACS_{01}** and **ACS_{02}** derivatives presented significant antileishmanial activity, with better performance than the reference drugs (tri and pentavalent antimonials), with respective IC_{50} values of 9.60±3.19 and 10.95±3.96 μM. Additionally, these two derivatives were effective against antimony-resistant *L. (*L.*) amazonensis* strains. In addition, binding and fragmentation DNA assays were performed. It was observed that the antileishmanial activity of **ACS_{01}** is not associated to DNA fragmentation of the promastigote forms. However, it interacted with DNA with a binding constant of 10^4 M^{-1}. In partial least-squares (PLS) studies, it was observed that the most active compounds (**ACS_{01}** and **ACS_{02})** showed lower values of amphiphilic moment descriptor, but there was a correlation between the lipophilicity of the molecules and antileishmanial activity. Furthermore, the docking molecular studies showed interactions between thiophene-acridine derivatives and the active site of pyruvate kinase enzyme with the major contribution of asparagine 152 residue for the interaction with thiophene moiety. Thus, the results suggested that the new thiophene-acridine derivatives are promising molecules as potential drug candidates.

Keywords: Leishmaniasis; 2-amino-thiophene; acridine; DNA binding; molecular docking.

1. Introduction

Neglected Tropical Diseases (NTDs) are a group of diverse contagious diseases that occur under tropical and subtropical climates in countries with precarious conditions, constituting a severe public health concern. Among the NTDs, leishmaniasis stands out for having the second highest incidence parasitism in the world, surpassed only by malaria, with a high level of mortality and morbidity [1,2,3].

Currently, the treatment applied to leishmaniasis is based on chemotherapy, although the available drugs are limited and most cause severe toxic side effects. Another concern is the increasing resistance developed by the parasite, diminishing the efficacy of the drugs, being necessary the discovery of new promising molecules to antileishmanial drugs [4].

The strategy of molecular hybridization, among the medicinal chemistry techniques, presents potential to the planning and developing of new drugs. This technique is based on the combination of specific structural characteristics of different bioactive moieties in order to produce new compounds, which displays better target affinity and biological efficacy when compared to its precursors. The new hybrid derivatives could also present a modified selectivity profile, as well as diminishing the undesirable side effects [5].

A lead chemical structure that have been explored for the synthesis of new active compounds is the acridine ring, by the condensation with different lateral chemical chain [6]. The resulting acridine derivatives are particularly interesting because the wide array of biological activities described in the literature such as antitumor, antimicrobial, anti-inflammatory, anti-malarial, anti-alzheimer and antitrypanosomal [6-12]. One of the main mechanisms that characterize biological activity of these compounds is attributed to the planarity of its aromatic structures, which can intercalate on the double helix of DNA and thus interfere in cellular and enzymatic functions [13-17].

Studies have reported the antileishmanial activity of acridine derivatives. Di Giorgio et al. [18] synthetized 6-mono-substituted and 3,6-di-substituted acridine derivatives and verified the anti-amastigote activity (1.1 µM) on *L. (L.) infantum*. Wong et al. [19] synthesized a series of compounds from quinacrine, an acridine analogous, and verified that these compounds restored the sensibility of *L. (L.) donovani* and *L. (L.) enrietti* to pentamidine, and that this action mechanism can be mediated by multiple targets.

Another class of compounds with antileishmanial potential are the 2-amino-thiophene derivatives. Rodrigues et al. [20] evaluated the effect of 2-amino-cycloalkyl[*b*]thiophene-carbonitrile derivatives on *L. (L.) amazonensis*. All tested compounds were active against the two forms of the parasite, presented low toxicity to murine macrophages and erythrocytes with inhibition of trypanothione reductase activity as suggested mechanism of action. Félix et al. [21] studied the importance of the molecular hybridization of 2-amino-thiophene and indole nuclei, evaluating the potential of the new hybrid compounds and verified that the majority of the compounds exhibited significant antileishmanial activity (IC_{50} < 10 µg/mL), and that the compounds were less toxic that the reference drugs (tri and pentavalent antimonials). Based on the previous works, here it was proposed the synthesis of new compounds by linkage of acridine and thiophene rings and evaluation of the antileishmanial activity.

Additionally, the enzyme pyruvate kinase has been extensively studied as a biological target for drug candidates, as it is important for the survival of the parasite [22]. Trypanosomatids, in the case of the parasites of the genus *Leishmania*, depend only on the

glycolytic pathway for ATP generation [23]. Thus, inhibition of this enzyme would cause cell death [24].

The present study described the synthesis of eight new thiophene-acridine hybrid compounds and the antileishmanial activity on promastigote forms of *L. (L.) amazonensis*. We also evaluated their cytotoxicity on human erythrocytes, and the action mechanism profile through DNA interaction and fragmentation assays, chemometric studies and molecular docking.

2. Experimental

2.1. Material and Methods

All reagents were commercial and used without further purification. Chromatography was performed on silica gel (60-120 mesh and 100-200). All reactions were monitored by thin layer chromatography (TLC) on Fluka Analytical silica gel thickness 0.2 mm plates with fluorescent indicator 254 nm and the disclosures were made by UV light (254 or 365nm). Fusion bands of the synthesized molecules were determined in open capillaries on the unit Quimis® Model Q-340M apparatus and were not corrected. The Nuclear Magnetic Resonance spectra of Hydrogen and Carbon were obtained on Agilent-NMR spectrometer, mod. Mercury Plus multinuclear 300MHz, magneto-NMR OXFORD 300 (operating at 400 or 300 MHz for ^{1}H and 100 or 75 MHz for ^{13}C) using DMSO-*d6* as solvent and tetramethylsilane (TMS) as internal standard. The processing of the spectra was done in MestReC 4.8.6.0 software. Chemical shifts are reported in parts per million. The multiplicities are reported as follows: singlet (s), doublet (d), doublet of doublet (dd), triplet (t) and multiplet (m). Infrared spectra were obtained with KBr discs on IRPrestige-21 spectrometer. The data were processed with Origin 8.0 software. The measures the exact masses of the molecular ions were obtained on a Shimadzu electrospray LC / MS-IT-TOF in a positive way. UV–Vis spectra were measured on an Ultraspec 3000 PRO UV–Visible spectrophotometer (Biochrom Ltd., Cambridge, UK) and fluorescence spectra on a JASCO FP-6300 (Jasco Corporation, Tokyo, Japan) spectrofluorometer.

The 6,9-Dichloro-2-methoxy-acridine (CAS 8638-4) was obtained commercially (Aesar® Alpha). The nucleus thiophen were obtained by Gewald classical reaction, and the condensed ring acridine were: **5CN**: 2-Amino-5,6-dihydro-4H-cyclopenta[b]thiophene-3-carbonitrile; **6CN**: 2-Amino-4,5,6,7-tetrahydro-benzo[b]thiophene-3-carbonitrile; **7CN**: 2-Amino-5,6,7,8-tetrahydro-4H-cyclohepta[b]thiophene-3-carbonitrile; **8CN**: 2-Amino-4,5,6,7,8,9-hexahydro-cycloocta[b]thiophene-3-carbonitrile; **6EST**: 2-Amino-4,5,6,7-

tetrahydro-benzo[b]thiophene-3-carboxylic acid ethyl ester; **7EST**: 2-Amino-5,6,7,8-tetrahydro-4H-cyclohepta[b]thiophene-3-carboxylic acid ethyl ester; **6AMD**: 2-Amino-4,5,6,7-tetrahydro-benzo[b]thiophene-3-carboxylic acid amide. All these compounds were obtained and characterized by our group, as previously reported [25, 26]. The acridine-9-carboxaldehyde was obtained with the methodology described by Barros et al. [7] and obtained satisfactorily.

2.2. General procedure for synthesis of new thiophene-acridine hybrids (ACT_{01})

The mixture of acridine-9-carboxaldehyde (**AC_{02}**) (1 equivalent) and the thiophene derivative 5CN in anhydrous ethanol (10 mL) was stirred at room temperature for 4-6 h. The product formation was accompanied by TLC with eluting system *n*-hexane/AcOEt 7:3. Since the reaction was complete, the material was filtered and washed with cold ethanol (20 mL) to give pure crystals.

2.2.1. 2-((acridin-9-ylmethylene)amino)-5,6-dihydro-4H-cyclopenta[b]thiophene-3-carbonitrile (ACT_{01})

Brown solid. Formula: $C_{22}H_{15}N_3S$; Yield: 58.6%; Melting point: 192 ºC; R*f* 0.57 (*n*-hexane/AcOEt 7:3). IR (KBr. cm^{-1}): 3446,79; 2846.93(=C-H); 2218.13 (C≡N); 1830.44; 1406.10; 1159.21; 945.11; 752.23; NMR ^1H (DMSO-d_6, 400 MHz, δ ppm): 9.73 (1H, s); 8.92 (2H, d, *J*= 8.7 Hz); 8.36 (2H, d, *J*=8.7 Hz); 7.85 (2H, dt, J_1= 8.7Hz, J_2=1.2 Hz); 7.72 (2H, dt, J_1= 8.7 Hz, J_2= 1.2Hz); 3.03 (2H, t, J_1= 14.4Hz, J_2= 7.2Hz); 2.95 (2H, t, J_1= 14.7 Hz, J_2=7.5 Hz); 2.60 (2H, q, J_1= 14.7 Hz, J_2= 7.2 Hz).

2.3 General procedure for synthesis of new thiophene-acridine hybrids (ACS)

The compounds 6,9-Dichloro-2-methoxy-acridine (1 equivalent) and thiophene derivatives in anhydrous ethanol (10 mL) were stirred at 60 ° C for 4-6 h. The product formation was accompanied by TLC with eluting system *n*-hexane/AcOEt 7:3. Since the reaction was complete, the material was filtered and washed with cold ethanol (20 mL) to give pure crystals.

2.3.1. 2-(6-chloro-2-methoxy-acridin-9-ylamino)-5,6-dihydro-4H-cyclopenta[b]- thiophene-3-carbonitrile (ACS_{01})

Beige solid. Formula: $C_{22}H_{16}ClN_3OS$; Yield: 87%; Melting point: 196 ºC; R*f* 0.56 (*n*-hexane/AcOEt 7:3). IR (KBr. cm^{-1}): 3392.78 (NH); 2208.49 (C≡N); 1631.77 (C=C); 1255.65

and 1032.57 (Ar-O-C); 936.97; NMR ^{1}H (DMSO-d_6, 400 MHz, δ ppm): 12.04 (1H, s, NH); 8.19 (1H, d, CH aromatic, J= 9.6Hz); 8.15 (1H, d, CH aromatic; J= 9.2 Hz); 7.84 (1H, d, CH aromatic, J= 9.2Hz); 7.58 – 7.52 (1H, m, CH aromatic); 7.40 (1H, dd, CH aromatic; J_1= 8.8Hz, J_2= 2.4Hz); 7.22 (1H, dd, CH aromatic, J_1= 8.8 Hz, J_2= 2.0 Hz); 3.84 (3H, s, OCH_3); 2.89 (2H, t, cycloalkyl, J_1= 13.6Hz, J_2= 6.8Hz); 2.74 (2H, t, cycloalkyl, J_1= 14Hz, J_2= 6.8Hz); 2.36 (2H, q, cycloalkyl, J_1= 14.4Hz, J_2= 7.4Hz; NMR ^{13}C (DMSO-d_6. 100 MHz, δ ppm): 26.88; 27.93; 29.64; 55.43; 104.93; 113.96; 116.20; 116.91; 117.42; 119.27; 120.46; 123.51; 124.41; 127.73; 128.24; 135.40; 137.52; 141.07; 142.54; 153.17; 154.27; 155.25. HRMS *m/z* $[M + H]^+$: calculated for $C_{22}H_{16}ClN_3OS$: 406.070; found: 406.078.

2.3.2. 2-(6-Chloro-2-methoxy-acridin-9-ylamino)-4,5,6,7-tetrahydro-benzo[b]- thiophene-3-carbonitrile (ACS_{02})

Mustard solid. Formula: $C_{23}H_{18}ClN_3OS$; Yield: 94.9%; Melting point: 237 ºC; R*f* 0.69 (chloroform/methanol 9:1). IR (KBr, cm^{-1}): 3329.13 (NH); 2941.44 (CH); 2221.99 (C≡N); 1631.77 (C=C); 1438.89; 1234.44 and 1085.92 (Ar-O-C); 933.54 (aromatic); NMR ^{1}H (DMSO-d_6, 300 MHz, δ ppm): 12.04 (1H, NH); 8.13 (1H, d, CH aromatic, J= 9.6Hz); 7.92-7.84 (2H, m, CH aromatic); 7.60-7.51 (2H, m, CH aromatic); 7.40 (1H, d, CH aromatic, J= 7.8Hz); 3.83 (3H, s, OCH_3); 2.65 (2H, s, cycloalkyl); 2.34 (2H, d, cycloalkyl, J= 22.5Hz); 1.73 ppm (4H, q, cycloalkyl, J_1= 22.8Hz, J_2= 4.2Hz); NMR ^{13}C (DMSO-d_6, 75 MHz, δ ppm): 21.67; 22.73; 24.04; 24.11; 55.20; 104.96; 114.47; 116.21; 117.13; 119.29; 120.29; 121.03; 122.95; 124.45; 127.98; 128.27; 133.00; 135.26; 135.62; 137.74; 139.81; 141.07; 154.30. HRMS *m/z* $[M + H]^+$: calculated for $C_{23}H_{18}ClN_3OS$: 420.085; found: 420.085.

2.3.3. 2-(6-Chloro-2-methoxy-acridin-9-ylamino)-5,6,7,8-tetrahydro-4H-cyclohepta[b]-thiophene-3-carbonitrile (ACS_{03})

Orange solid. Formula: $C_{24}H_{20}ClN_3OS$; Yield: 94.3%; Melting point: 194 ºC; R*f* 0.72 (chloroform/methanol 9:1). IR (KBr, cm^{-1}): 3649.31 (NH); 3275.12; 2922.15 (CH); 2638.62; 2204.63 (C≡N); 1627.92 (C=C); 1552.68; 1271.08 and 1083.99 (Ar-O-C); 929.68 (aromatic); NMR ^{1}H (DMSO-d_6, 300 MHz, δ ppm): 11.93 (1H, s, NH); 8.07 (1H, d, CH aromatic, J = 8.7 Hz); 7.59 (1H, d, CH aromatic, J= 2.4 Hz); 7.54 (1H, d, CH aromatic, J= 4.8); 7.50 (1H, d, CH aromatic, J= 4.2 Hz); 7.43 (1H, m, CH aromatic, J= 4.2 Hz); 7.23 – 7.18 (1H, m, CH aromatic); 3.65 (3H, OCH_3, s,); 2.70 (2H, t, cycloalkyl, J_1=9.9 Hz, J_2=4.5Hz); 2.60 (2H, t, cycloalkyl, J_1=9.9 Hz, J_2=4.5Hz); 1.82- 1.54 (6H, m, cycloalkyl); NMR ^{13}C (DMSO-d_6, 75 MHz, δ ppm): 26.94; 27.03; 28.74 (2C); 31.34; 54.93; 105.66; 115.59; 116.21; 116.54;

116.88; 119.27; 119.82; 121.06; 121.79; 124. 48; 128.41; 129.89; 134.87; 135.59; 137.07; 137.65; 139.96; 154.06. HRMS *m/z* [*M* + H]$^+$: calculated for $C_{24}H_{20}ClN_3OS$: 434.101; found: 434.103.

2.3.4. 2-(6-Chloro-2-methoxy-acridin-9-ylamino)-4,5,6,7,8,9-hexahydro-cycloocta[b]-thiophene-3-carbonitrile (ACS_{04})

Brown solid. Formula: $C_{25}H_{22}ClN_3OS$; Yield: 89.3%; Melting point: 253 ºC; R*f* 0.67 (chloroform/methanol 9:1). IR (KBr, cm^{-1}): 3446.79 (NH); 2926.01(CH); 2218.13 (C≡N); 1625.99 (C=C); 1492.90; 1234.44 and 1080.13 (Ar-O-C); 931.61; NMR ^{1}H (DMSO-d_6, 400 MHz, δ ppm): 11.87 (1H, s, NH); 8.21 (1H, d, CH aromatic, *J*=8.8 Hz); 7.61 (1H, d, CH aromatic, *J*=3.2Hz); 7.55 (1H, d, CH aromatic, *J*= 1.6Hz); 7.52 (1H, d, CH aromatic, *J*=9.2Hz); 7.42 (1H, dd, CH aromatic, *J*=9.2Hz, *J*=3.2 Hz); 7.22 (1H, dd, CH aromatic, *J*= 8.8 Hz, *J*=2.0 Hz); 3.85 (3H, s, OCH_3); 2.78 (2H, t, cycloalkyl, *J*= 6.0 Hz); 2.64 (2H, t, cycloalkyl, *J*=12Hz, *J*=6.0Hz); 1.60 (4H, s, cycloalkyl); 1.43 (4H, s, cycloalkyl); NMR ^{13}C (DMSO-d_6, 100 MHz, *δ* ppm): *δ*=22.10; 23.14; 24.31; 25.30 (3C); 55.37; 104.96; 114.84; 116.21; 119.29; 121. 05; 124.48; 127.15; 127.34; 128.28; 128.39; 129.47; 129.51; 133.81; 139.84; 141.07; 154.31; 175.54; HRMS *m/z* [*M* + H]$^+$: calculated for $C_{25}H_{22}ClN_3OS$: 448.117; found: 448.114.

2.3.5. 2-(6-Chloro-2-methoxy-acridin-9-ylamino)-4,5,6,7-tetrahydro-benzo[b]thiophene-3-carboxylic acid ethyl ester (ACS_{05})

Orange solid. Formula: $C_{23}H_{20}ClN_3O_2S$; Yield: 81.5%; Melting point: 245 ºC; R*f* 0.68 (chloroform/methanol 9:1). IR (KBr, cm^{-1}): 3404.36 (NH); 2937.58 (CH); 2636.69; 2360.87; 1707.00 (C=O ester); 1489.04; 1274.94 and 1029.98 (Ar-O-C); 937.40; NMR ^{1}H (DMSO-d_6, 300 MHz, *δ* ppm): 11.91 (1H, s, NH); 8.20 (1H, d, CH aromatic, *J*= 8.1Hz); 7.72 (1H, d, CH aromatic, *J*= 3.0Hz); 7.55-7.54 (1H, m, CH aromatic); 7.51-7.47 (1H, m, CH aromatic); 7.42 (1H, dd, CH aromatic, *J*= 8.7Hz, *J*= 3.0Hz); 7.22 (1H, dd, CH aromatic, *J*= 8.7Hz, *J*=1.8Hz); 4.13 (2H, q, CH_2 ester, *J*= 14.1Hz, *J*= 6.9Hz); 3.85 (3H, s, OCH_3); 2.58 (2H, d, cycloalkyl, *J*= 6.0Hz); 2.39 (2H, d, cycloalkyl, *J*= 5.1Hz); 1.77-1.64 (4H, m, cycloalkyl); 0.67 (3H, t, CH_3 ester, *J*= 14.1Hz, *J*=6.9Hz); NMR ^{13}C (DMSO-d_6, 75 MHz, *δ* ppm): 11. 37; 22.39; 23.91; 24.49; 26.50; 55.40; 59.60; 104.97; 112.30; 115.47; 116.22; 119.30; 121.08; 122.00; 122.80; 124.51; 127.55; 128.31; 132.10; 134.22; 135.63; 137.62; 138.40; 141.08; 154.34. HRMS *m/z* [*M* + H]$^+$: calculated for $C_{23}H_{20}ClN_3O_2S$: 467.111; found: 467.110.

2.3.6. 2-(6-Chloro-2-methoxy-acridin-9-ylamino)-5,6,7,8-tetrahydro-4H-cyclohepta[b] thiophene-3-carboxylic acid ethyl ester (ACS_{06})

Orange solid. Formula: $C_{25}H_{23}ClN_2O_3S$; Yield: 44.8%; Melting point: 211 ºC; R*f* 0.71 (chloroform/methanol 9:1). IR (KBr, cm^{-1}): 3404.36 (NH); 2912.51 (CH); 2692.62; 1712.78 (C=O ester); 1514.12(C=C); 1271.08 and 1029.98 (Ar-O-C); 937.40; NMR ^{1}H (DMSO-d_6, 300 MHz, δ ppm): 11.90 (1H, s, NH); 8.20 (1H, d, CH aromatic, *J*=8.1 Hz); 7,60 (1H, d, CH aromatic, *J*= 3.0 Hz); 7.55 (1H, d, CH aromatic, *J*= 1.8Hz); 7.52 (1H, d, CH aromatic, *J*= 9.3 Hz); 7.42 (1H, dd, CH aromatic, J_1= 9.3 Hz; J_2= 3.0 Hz); 7.22 (1H, dd, CH aromatic, *J*= 9.0 Hz; *J*= 1.8 Hz); 4.16 (2H, q, CH_2 ester, J_1=14.1 Hz, J_2= 6.9 Hz); 3.85 (3H, s,OCH_3); 3.42 (2H, s, cycloalkyl); 2.90 - 2.83 (2H, m, cycloalkyl); 1.90 - 1.50 (6H, m, cycloalkyl); 0.62 (3H, t, CH_3 ester, J_1= 14.1 Hz, J_2= 7.2 Hz); NMR ^{13}C (DMSO-d_6, 75 MHz, δ ppm): 14.37; 22.39; 23.91; 24.49; 26.50; 55.40; 59.60; 104.97; 112.30; 115.47; 116.22; 119.30; 121.08; 122.00; 122.80; 124.51; 127.55; 128.31; 132.10; 134.22; 135.63; 137.62; 138.40; 141.08; 154.34. HRMS *m/z* $[M + H]^+$: calculated for $C_{25}H_{23}ClN_2O_3S$: 481.127; found: 481.002.

2.3.7. 2-(6-Chloro-2-methoxy-acridin-9-ylamino)-4,5,6,7-tetrahydro-benzo[b]thiophene-3-carboxylic acid amide (ACS_{07})

Yellow solid. Formula: $C_{26}H_{25}ClN_2O_3S$; Yield: 86.2%; Melting point: 212 ºC; R*f* 0.61 (*n*-hexane/AcOEt 7:3). IR (KBr, cm^{-1}): 3429.43 (NH); 3138.18; 2939.65; 2362.79; 1635.63 (C=O amide); 1492.90; 1244.08; 860.25; 835.17 (aromatic); NMR ^{1}H (DMSO-d_6, 300 MHz, δ ppm): δ= 11.86 (1H, s, NH); 8.21 (1H, d, CH aromatic, *J*= 8.1Hz); 7.94-7.86 (1H, m CH aromatic); 7.65-7.51 (2H, m, CH aromatic); 7.41 (1H, d, CH aromatic, *J*= 6.6Hz); 7.21 (1H, d, CH aromatic, *J*= 6.9Hz); 4.02 (1H, s, NH amide); 3.85 (3H, s, OCH_3); 3.71 (1H, s, NH amide); 2.68 (4H, s, cycloalkyl); 1.77 (4H, s, cycloalkyl); NMR ^{13}C (DMSO-d_6, 75 MHz, δ ppm): 22.62 (2C); 24.04; 24.11; 55.34; 105.03; 114.47; 116.14; 117.13; 119.14; 120.97; 121.03; 122.95; 124.36; 127.98; 128.22; 135.56; 133.02; 137.74; 139.9; 141.05; 154.28; 166.01. HRMS *m/z* $[M + H]^+$: calculated for $C_{26}H_{25}ClN_2O_3S$: 438.096; found: 438.100.

2.4. Antileishmanial activity evaluation

2.4.1. Parasites and in vitro maintenance

Promastigote forms of *L. (L.) amazonensis* (IFLA/BR/67/PH8) used in the assays coming from cultures of Bank Institute of Biological Sciences at University Federal de Minas Gerais, Brazil. They were cultivated in test tubes containing NNN (Novy-McNeal-Nicolle) blood agar culture medium associated to Schneider liquid medium (Sigma, USA),

supplemented by 20% Fetal Bovine Serum (FBS) and 1% streptomycin (100 µg/mL) and penicillin (100 U.I./mL). Cells were incubated at 25±1 °C and the medium was changed weekly to maintain cellular viability.

2.4.2. Antipromastigote activity evaluation and determination of 50% growth inhibition concentration (IC_{50})

For the *in vitro* tests, compounds were diluted in DMSO (Sigma - Aldrich ™, St Louis, USA) to prepare a stock solution, and posteriorly diluted in Schneider liquid medium to final work solutions (5-200 µg/mL). The final DMSO concentration in culture did not overpassed 1.0%, concentration that does not present cytotoxicity for promastigote forms of *Leishmania* sp. and human erythrocytes.

The determination of growth inhibition of promastigote forms of *L. (L.) amazonensis* by the studies substances was performed in screw capped test tubes containing 1.0 mL of Schneider medium supplemented with 20% FBS and streptomycin (100 µg/mL) and penicillin (100 UI/mL). The density of 1 x 10^6 of *L. (L.) amazonensis* promastigotes/mL in logarithmic growth phase were added to the test tubes in absence (control) and presence of different concentrations of the evaluated substances.

After 72 hours of incubation at 25 ºC±1, samples of each culture were obtained, diluted in isotonic solution (10.5 g citric acid, 7 g NaCl, 15 mL formaldehyde in 1 L distilled water), analysed and quantified directly under optic microscope in a Neubauer chamber. The *L. (L.) amazonensis* cultures were evaluated for their sensitivity to the pentavalent antimony Glucantime® (Aventis Pharma ™, SP, Brazil), Potassium antimonyl tartrate trihydrate (trivalent antimony source) (Sigma-Aldrich – code: 383376) and Amphotericin B ® (Cristália, SP, Brazil), used as reference drugs. The assays were performed in duplicated and repeated at least three times. The control cultures, whose growth was considered 100%, were maintained in drug absence and the calculation of 50% growth inhibition concentration (IC_{50}) for each compound was obtained by comparison to the control cultures. The 50% inhibitory concentration (IC_{50}) was calculated by Probit analysis (SPSS for Windows 13.0).

2.5. Hemolytic activity evaluation

The hemolytic activity was evaluated by incubation of the thiophene-acridine derivatives diluted in PBS solution with 80 µL of a 5% suspension of human erythrocytes (O^+) during one hour at 37 °C. The reaction was stopped by adding 200 µL of PBS solution, followed by centrifugation at 1,000 g for 10 minutes. The supernatant was collected and

cellular lysis was measured via spectrophotometer (540 nm). The absence of hemolysis and total hemolysis (positive control) were determined by substituting the solution containing the tested substances (25-800 µg/mL) by an equal volume of PBS or Milli-Q sterile water, respectively. The results were determined by comparing the percentage of hemolysis to the positive control (100% hemolysis). All assays were performed in triplicates at least twice [20]. This study was approved by the Ethics Committee of the Human Health Sciences Center Research (CCS), UFPB (Protocol number 0511/15, CAAE: 49005615.7.0000.5188), Brazil.

2.6. Determination of selectivity index

The antipromastigote and human erythrocytes hemolysis data were used for the IC_{50} (concentration capable of inhibit 50% of parasitic growth) and HC_{50} (concentration needed to induce lysis in 50% of the erythrocytes) estimation, respectively. These data allowed to calculate the Selectivity Index (SI) by the ratio between HC_{50} and IC_{50} (SI: HC_{50}/ IC_{50}). The SI indicates if the tested compound is more selective for the parasite (*Leishmania*) than to the mammal cells for *in vitro* assays performed. The compounds which presented higher SI values were selected for posterior assays.

2.7. Evaluation of antipromastigote activity against Sb (III) resistant strains

The compounds **ACS_{01}** and **ACS_{02}** (with highest SI) were selected for evaluation the activity against *L. (L.) amazonensis* strains resistant to trivalent antimonial (22.5 times more resistant than wild). For this analysis, it was used the same method described in the item 2.4.2.

2.8. DNA fragmentation analysis by agarose gel electrophoresis

The **ACS_{01}** and **ACS_{02}** were selected to evaluate its capacity of causing fragmentation of the DNA parasite as an indication of apoptosis. Promastigote forms of *L. amazonensis* in logarithmic phase of growth were incubated in absence (negative control) and presence of **ACS_{01}** at concentration of 1, 2 and 4 higher than IC_{50}. The cultures were incubated overnight at 25 ± 1°C, followed by DNA extraction. The *Leishmania* DNA extraction was performed using the chloroform/phenol method [20]. The concentration and degree of purity of the DNA extracted from the *L. amazonensis* cultures were estimated by spectrophotometer (Thermo Scientific NanoDrop 2000). The DNA with GelRed Nucleic Acid Gel Stain 1:500 (10.000x Biotium®) colorant was added to 1% agarose gel (Gibco, USA) and the electrophoresis was performed in TBE (Tris/Borato/EDTA) solution at 60 V, 50 mA. After the electrophoresis,

the gels were analysed under UV transilluminator **(**ImageMaster®). The assays were performed in duplicates and repeated once.

2.9. DNA binding assay

2.9.1. UV-Vis Absorption Measurements

All experiments involving interactions of derivatives and ctDNA were carried out in 10 mM Tris-HCl buffer (pH 7.6). The solution of ctDNA in Tris buffer was sonicated for 5 min and the DNA concentration was determined using the molar extinction coefficient 6.600 M^{-1} cm^{-1} at 260 nm [27]. The purity of DNA was determined by monitoring the value of the A_{260}/A_{280} ratio. DNA concentration was expressed as micromolar equivalents of the base pairs. Compounds **ACS_{01}** and **ACS_{02}** were dissolved in DMSO at a concentration of 1 mM (stock solution) from which working solutions of concentrations ranging from 10 to 50 μM were prepared by dilution using Tris buffer. After compound concentration optimization, the absorption spectral titration experiment was performed by keeping the compound concentration (30 μM) while varying the DNA concentration (0-100 μM bp). All measurements were performed at 25 °C in a rectangular quartz cuvette with a 1-cm path length. The intrinsic binding constant (Kb) with ctDNA was obtained by fitting the data to Equation (1) [28]:

$$[DNA]/(\varepsilon_a - \varepsilon_f) = [DNA]/(\varepsilon_b - \varepsilon_f) + 1/K_b\,(\varepsilon_b - \varepsilon_f) \qquad (1)$$

where ε_a, ε_b and ε_f are the apparent, bound, and free extinction coefficients for each compound, respectively. Plot fitting of exponential equation $[DNA]/(\varepsilon_a - \varepsilon_f)$ *vs.* [DNA] was used for obtaining the K_b values. The binding data were fitted using the Origin 8.0 software.

2.9.2. Fluorescence Measurements

All fluorescence measurements of non-bound and ctDNA-bound derivatives were performed with solution concentration of 10 μM in 10 mM Tris buffer, pH 7.6. Emission spectra were recorded in the region 440–600 nm using an excitation wavelength of 417 nm for both compounds. All measurements were performed at 25 °C in a rectangular quartz cuvette with a 1-cm path length. Fluorescence intensities were expressed in arbitrary units. Fluorescence titrations were conducted by the addition of increasing amounts of ctDNA (0–100 μM bp) directly into the cell containing solutions of the derivatives. Fluorescence intensities of compound solutions exposed to different ctDNA concentrations were used to calculate the relative fluorescence decreasing by I/I_0 that are fluorescence intensities in the presence and absence of ctDNA.

2.10. Chemometric Studies

2.10.1. VolSurf Descriptors

Three-dimensional structures (3D) were used as input data in the VolSurf+ program v. 1.0.7, and were subjected to molecular interaction fields (MIF) to generate descriptors using the following probes: N1 (amide nitrogen-hydrogen bond donor probe), O (carbonyl oxygen-hydrogen bond acceptor probe), H_2O (water probe), and DRY (hydrophobic probe). Additional non-MIF-derived descriptors were generated to create a total of 128 descriptors [29]. VolSurf descriptors have been previously used to predict the activity of against neglected protozoan diseases [30, 31].

2.10.2. Partial Least-Squares (PLS) model

PLS regression were applied to construct models considering a training set of 16 compounds [32]. The number of latent variables (LV), as well as original variables, were selected by using a Variable Influence on Projection (VIP) plot, together with the plot that reports, for each PLS component, the explained variance in fitting (R^2) and the explained variance in predicting (Q_{cv}^2; cross-validation by leave-one-out). The VIP (Variable Importance in Projection) plot condenses the importance of the independent variables, either for the explained variances among themselves, or for the dependent variable of the PLS model. The model with the highest value of cross-validation correlation coefficient (Q_{cv}^2) was selected.

2.10.3. Molecular Docking

L. amazonensis and *L. mexicana* share several genotypic features [33], therefore, the structures of pyruvate kinase and arginase in complex, respectively, with 2(s)-amino-6-boronohexanoic acid (ABH, PDB ID 4IU0) [33], and suramin in (PDB ID 3PP7) [34] from *L. mexicana* were downloaded from the protein data bank (http://www.rcsb.org/pdb/home/home.do). The structures of thiophene derivatives were submitted to molecular docking using the Molegro Virtual Docker, v. 6.0.1 (MVD) [35]. All the water molecules were deleted from the enzyme structure, and the enzyme and compound structures were prepared using the same default parameter settings in the same software package (Score function: MolDock Score; Ligand evaluation: Internal ES, Internal HBond, Sp2-Sp2 Torsions, all checked; Number of runs: 10 runs; Algorithm: MolDock SE; Maximum Interactions: 1500; Max. population size: 50; Max. steps: 300; Neighbor distance factor: 1.00; Max. number of poses returned: 5). The docking procedure was performed using

a GRID of 15 Å in radius and 0.30 in resolution to cover the ligand-biding site of both pdb files. Templates with features expected to be relevant for ligand binding extracted for both ligands were generated to perform docking. The Moldock score [GRID] algorithm was used as the score function, and the Moldock search algorithm was used [35]. Docking was validated redocking the original ligand rosiglitazone in active site of enzymes as observed in crystallography pdb file (PDB ID 4IU0 and 3PP7) [34, 36].

2.11. Statistical analysis

The data obtained were presented as mean±standard error of the mean (SEM). Student'st-test was used to evaluate the individual data significance, and one-way analysis of variance (ANOVA) for comparison between groups. For statistical analysis GraphPad Prism software version 5.0 for Windows (GraphPad Software, San Diego, CA, USA) was used. Only values of $p \leq 0.05$ were considered as significant.

3. Results and discussion

3.1 Synthesis of thiophene-acridine compounds

The synthesis of 2-amino-thiophene the thiophene-acridine compounds is presented in Scheme 1. The 2-amino-thiophene derivatives (**5CN, 6CN, 7CN, 8CN, 6EST, 7EST, 6AMD**) were obtained using the classic Gewald reaction, as previously described [25, 26]. The thiophene-acridine derivatives were obtained through linkage reactions between different 2-amino-thiophene compounds and acridine moieties, via nucleophilic aromatic substitution, resulting in the final compounds **ACS_{01}** to **ACS_{07}** and **ACT_{01},** with good efficiency.

All new thiophene-acridine derivatives presented over 44% yields and their physicochemical characteristics and structures were determined by spectrometric data according to the structures proposed. The ^{1}H and ^{13}C NMR and HRMS data are available in supporting material which demonstrated that all structures were confirmed.

The ^{1}H NMR of the ACS series shows signals (δ) between 1.43 and 3.42 ppm that corresponded to cycloalkyl to all the compounds. The linkage between the amine function and the 6,9-dichloro-2-methoxy-acridine core conducted to a substituted amine (NH-Ar) with chemical shifts signals between 11.86 - 12.4 ppm, observed to all compounds which prove the linkage between the moieties. It was also possible to observe singlet signals between 3.65 and 3.85 ppm, corresponding to the methoxy chemical shifts [18], and acridine peaks between

7.22 and 8.21 [17]. In addition, for the **ACS$_{05}$** and **ACS$_{06}$**, it was observed the chemical shifts of the ester function between 0.62 - 0.67 (CH_3) and 4.13 - 4.16 (CH_2) ppm [37].

The IR spectre results demonstrated the carbonitrile from the amide function (HNC=O) in **ACS$_{07}$** by absorption at 1635 cm^{-1}, according to the absorption values (1630 - 1690 cm^{-1}). The NH_2 function from the amide was observed at 3138 cm^{-1}. To all compounds, the absorption band for the aromatic ether group (Ar-O-C) was between 1029 - 1085 and 1234 - 1271 cm^{-1} [37]. On regard to the nitriles (CN), the absorption on the region was associated to axial deformation vibrations on the triple bonds occurring between 2204 - 2221 cm^{-1} [32, 33]. Regarding **ACS$_{05}$** and **ACS$_{06}$** derivatives, the ester function presented absorption of 1707 and 1712 cm^{-1}, respectively [37]. Moreover, HRMS confirmed the identity of all the synthesized compounds (see supporting material).

3.2 Biological activity

3.2.1 Cytotoxicity and antileishmanial activities

None of the new thiophene-acridine derivatives tested presented cytotoxicity against human erythrocytes up to the highest concentration evaluated (1000 µM), which characterized that the compounds obtained are no toxic to blood cells. In addition, it is important to note that Amphotericin B, a drug used in the current therapy of leishmaniasis, showed haemolytic activity (HC_{50} 24.25±2.52 µM), being more toxic than all the derivatives evaluated in this study [38]. It was observed that the addition of chemical groups to the compounds (nitrile, ester and amide), as well as the increase of the carbon numbers in the cycloalkyl group, did not alter the cytotoxicity of the new derivatives (Table 1).

Regarding antiparasitic activity, the 2-amino-thiophene, acridine-9-carboxyaldehyde and 6,9-dichloro-2-methoxy-acridine moieties were tested separately, as all are considered privileged structures, to check the success of the new compounds synthesised. All the moieties presented low activity on promastigote forms of *L. (L.) amazonensis*, presenting antileishmanial activity with IC_{50} values < 80 µM, with the exception of **AC02** and **8CN** (Table 1).

The linkage of acridine-9-carboxyaldehyde with 2-amino-thiophene moieties conducted to a loss of activity (IC_{50} > 500 µM). However, the new compounds obtained by the 6,9-dichloro-2-methoxy-acridine and the 2-amino-thiophene moieties favoured the antipromastigote activity, once they presented antileishmanial activity with IC_{50} between 9.62

and 69.11 µM. Also, some of the tested compounds presented higher activity than the tri and pentavalent antimonials (reference drugs), as seen by the IC_{50} values (Table 1).

It was observed that the size of the cycloakyl ring interferes in the antileishmanial activity, as the cyclopentane [**ACS_{01}** (IC_{50} 9.60±3.19 µM)] and cyclohexane [**ACS_{02}** (IC_{50} 10.95±3.96 µM)] presented higher activity than the cycloheptane [**ACS_{03}** (IC_{50} 32.26±5.50 µM)] and cyclooctane [**ACS_{04}** (IC_{50} 68.97±4.85 µM)]. Thus, these results suggest that the increase in the number of methylene carbon groups can cause increased lipophilic and steric effects, affecting the pharmacological response. In addition, the presence of the nitrile radical improved the biological activity of the compounds [**ACS_{02}** (IC_{50} 10.95±3.96 µM)], when compared to the compounds **ACS_{05}** and **ACS_{07}** [**ACS_{05}** (IC_{50} 26.55±3.98 µM) and **ACS_{07}** (IC_{50} 51.37±13.14 µM)], with ester and amide radicals, respectively. The importance of the nitrile group bound to heterocyclic nuclei was studied by McGeary et al. [39] where it was shown that this functionality would be related to a greater interaction with an enzymatic catalytic site and consequently a better biological response.

In attempt to evaluate the selective activity for the parasite by the new compounds, the cytotoxic against human erythrocytes was performed. The results demonstrated that all tested compounds were more toxic to the promastigote forms of *L. (L.) amazonensis* than to human erythrocytes. From the results, the selectivity indexes (SI) both to the reference drugs as well as for the new derivatives, were obtained. The SI values of the ACS series of thiophene-acridine compounds demonstrated better selectivity than the antimonials, with **ACS_{01}** and **ACS_{02}** presenting higher SI values than all reference drugs used, as shown in Table 1.

Based on the selectivity index, **ACS_{01}** and **ACS_{02}** derivatives were selected for further tests. The choice was based on the IC_{50} values of the compounds, as well as the absence of toxicity against erythrocytes and higher selectivity for the parasite. It was performed growth inhibition tests using parasite strains resistant to trivalent antimony (SbIII) and the values were similar to the ones obtained in sensitive strains, previously exposed to the same compounds (Table 2). The compound **ACS_{01}** presented IC_{50} of 14.83±0.44 µM for the resistant strains, compared to 14.04±1.46 µM for the sensitive strains. **ACS_{02}** presented IC_{50} of 16.36±1.72 µM for the resistant strains, with 16.05±1.38 µM for the sensitive ones. The results prove the efficacy of **ACS_{01}** and **ACS_{02}** derivatives on the chemotherapy when applied on strains resistant to the current therapy.

3.2.2 DNA assays

DNA interaction and fragmentation tests were performed to verify the possible action mechanism of the compounds, whereas 9-amino-6-chloro-2-methoxyacridine derivatives are well known as DNA intercalator [40]. It was performed the analysis of DNA binding *in vitro* with ctDNA by UV-vis absorption and fluorescence emission of **ACS$_{01}$** and **ACS$_{02}$** derivatives. Acridine derivatives present absorption and emissive properties due the chemical structure of fused aromatic rings [13]. Besides this, the planarity of acridine ring allows the intercalation between pair bases of DNA [15]. These characteristics have been widely used in several studies in order to establish the biological action mechanism of acridine derivatives after chemical modifications [14,17]. Based on this information, it was supposed that the effects of **ACS$_{01}$** and **ACS$_{02}$** on DNA could constitute one of the mechanism against *Leishmania.*

The interaction of **ACS$_{01}$** and **ACS$_{02}$** with ctDNA was monitored by spectrophotometric titrations in aqueous buffer [17]. The absorption spectra of **ACS$_{01}$** and **ACS$_{02}$** displayed absorption bands in the region of 350-600 nm (See supplementary material). The changes observed in the complexes absorption spectra in the presence of increasing concentration of ctDNA were used for determining the interaction of derivatives with duplex DNA. A red shift of the absorption maximum was observed upon addition of DNA for both compounds (9 and 24 nm for **ACS$_{01}$** and **ACS$_{02}$**, respectively), besides an increase of the absorption intensity. The absorption spectra of derivatives in the absence and presence of ctDNA are depicted in Figure 1.

The data of the spectrophotometric titrations were used to estimate the binding constants (Kb) according to the model of McGhee and von Hippel [27]. **ACS$_{01}$** and **ACS$_{02}$** derivatives bind to ctDNA with values of Kb = 10^4 M^{-1}. Typical Kb for intercalation complexes between organic dyes and DNA range from 1×10^4 to 1×10^6 M^{-1} [41]. Similar DNA binding constants were found by Lafayette et al. [14] for thiazacridine and imidazacridine derivatives. The 6-chloro-2-methoxy-acridine moiety found in our compounds (**ACS$_{01}$** and **ACS$_{02}$** derivatives), are of great biological importance since it is reported in the literature the possibility of interaction with DNA Zhang et al. [42] probably by the establishment of hydrogen bonding with this biomacromolecule. These results indicate that the substitution of acridine ring with chloro and methoxy moieties did not impair DNA interaction. Furthermore, it was not observed significant differences in DNA binding properties between **ACS$_{01}$** and **ACS$_{02}$** through spectrophotometric titrations.

The interaction of **ACS_{01}** and **ACS_{02}** with ctDNA it also was investigated by fluorescence spectroscopy. Both derivatives showed emissive properties with excitation and emission wavelengths at 417 and 463 nm, respectively (Figure 2). Fluorescence spectra were monitored at a fixed concentration of 10 μM of each derivative and different ctDNA concentrations. The fluorescence of both compounds was quenched upon binding to ctDNA bases, but the decrease in fluorescence emission of **ACS_{02}** was lower than those observed for **ACS_{01}**. This emission-quenching phenomenon confirms the interaction between the compounds and ctDNA [13,14], and indicates that the methoxy moiety influences the DNA interaction.

After to identify that **ACS_{01}** and **ACS_{02}** binding to ctDNA, a DNA fragmentation assay was carried to verify if the compounds would cause fragmentation besides DNA intercalation. The results demonstrated that the promastigote forms of the parasite treated with **ACS_{01}** did not presented DNA fragmentation (data not shown), with no DNA bands formation in any tested concentrations one, two and four times the IC_{50} compared to the positive control (Amphotericin B), with results like the negative control (untreated promastigotes). This result was similar to those described for 2-(acridin-9-ylmethylene)-*N*-phenylhydrazinecarbothioamide against human breast adenocarcinoma cells where the derivative did not promote DNA fragmentation of the treated cells [43].

Acridine derivatives are considered as DNA intercalators and inhibitor of essential cell replicative enzymes. In addition, these derivatives also have the capacity to be dual inhibitors, being potent in reducing resistance to multiple drugs through other mechanisms of action [44]. These evidences lead us to believe that the mechanism of death of the parasite is not associated with DNA fragmentation, but may be associated with the inhibition of enzymes critical for its survival. However, these mechanisms of action should be investigated in future tests.

3.2.3 PLS Studies

The dataset that was evaluated is composed by 16 thiophene derivatives - synthetic intermediate and final compounds - (See supplementary material). Auto scaling preprocess was applied to the PLS analysis using VolSurf descriptors as independent variables and pIC_{50} (-log IC_{50}), value concentration necessary to inhibition growth of 50% promastigote cells of *L. amazonensis,* as dependent variables. After the variable selection using the Variable Important Projection the PLS generated significant statistical measures (leave-one-out cross-

validation correlation coefficient, Q_{cv}^2 = 0.80; and the coefficient of determination, R^2 = 0.89), using only two latent variables (LV). The first LV explains 78.6 % and LV 28.5%, summarizing 87.1 % of the total variance of independent variables. Figure 3A shows that the model containing three LVs presented an increment in R^2 value, but the Q_{cv}^2 value began to decrease.

Visualizing the plot of experimental pIC_{50} values versus recomputed (Figure 3B) and predicted (Figure 3C) can be noticed that both depict the adjustment regarding a straight line of the points used for the calibration of the model and validation.

The coefficients plot (Figure 4A) shows the 12 variables selected and together with the loadings plot (Figure 4B), it is possible to notice that Amphiphilic moment (A) and Hydrophobic Integy moment, ID1 and ID3, are the main descriptors with a negative contribution to pIC_{50}. The 3D Dry-Acceptor-Acceptor (DRDRAC) shows low positive contribution to pIC_{50} values [29]. Analyzing the coefficients and the loadings plot of the selected descriptors, one realizes that the model extract the physical-chemical features that are undesirable for antileishmanial activity for this set.

The scores plot (Figure 5) differentiate the more active compounds **AC02**, **ACS_{01}** and **ACS_{02}** (in the first quadrant) from most inactive compound 8 (**6AMD**) localized in the third quadrant.

The Amphiphilic moment descriptor is defined as a vector pointing from the center of the hydrophobic domain to the center of the hydrophilic domain. The vector length is proportional to the strength of the amphiphilic moment. It is possible to check the association among higher values of this descriptor for the inactive compounds such **ACS**, **6CN** and **6AMD**. The most active compounds **AC_{02}**, **ACS_{01}** and **ACS_{02}** show lower values of Amphiphilic moment descriptor, therefore the symmetric distribution of hydrophobic and hydrophilic regions causes the near positioning of both center domain. Compound **6AMD** show two distinct hydrophilic and lipophilic regions on two different sides of the structure, on the other hand compound **ACS_{01}** these regions are distributed in such way that there is not formation of poles (Figure 6A) [29].

The Hydrophobic Integy moment ID1 and ID3 describe the unbalance between the center of mass of a molecule and the barycenter of its hydrophobic region generated at -0.2 and at -0.6 kcal/mol respectively. The symmetry of the hydrophobic region of the molecule is

significantly noticeable in the active compounds as it is possible to visualize in Figure 6B comparing compound **6AMD** and **AC_{02}**. The **6AMD** shows antisymmetric hydrophobic region, unlike compound **AC_{02}** [29].

Descriptor DRDRAC is a 3D (three-dimensional) pharmacophore descriptor. This kind of parameter is based on the triplets of pharmacophoric points descriptors. At first the atoms (points) of a structure are classified as Dry, H-bond donor and H-bond acceptor, then all possible triplet of distances between these atoms are generated. The DRDRAC descriptor is the maximum area (over all possible conformers) of the triangles derived from triplet Dry-Dry-Acceptor (H-bond acceptor).

3.2.4 Molecular Docking

For better understanding the chemical group influence on antileishmanial activity, molecular docking studies were performed [45]. It is worthwhile to highlight that for a neglected pathogen such as *Leishmania*, there are just a few representative structures of enzymes on the PDB, and only some of them have multiple structures (e.g., pyruvate kinase of *L. mexicana*) as demonstrated recently [46]. In our case, the analysis was focused on pyruvate kinase enzyme. Docking results of pyruvate kinase show a clear correlation among pIC_{50} values against *L. amazonensis* promastigote and MolDock energies of the set of compounds excluding compound 9 (**AC_{02}**) (r =-0.76, table 2 in supporting data). Analysing the compounds with pIC_{50} values above of 4.29 show energies lower than -107 kJ/mol, being minor than the ligand ABH (-99.18 kJ/mol). The results of the arginase show not only very low correlation, but positive (r =0.57, table 2 in supporting data), in other words, more active compounds have higher MolDock energies, therefore more instable interactions. Figure 7A shows interactions between compound **ACS_{01}** and the active site of pyruvate kinase. Residue asparagine 152 is responsible for the interaction with thiophene moiety. The compounds **ACS_{01}** to **ACS_{04}** almost show the same interactions in the pocket (Figure 7B). Even the dock energies of these compounds are similar, increasing the number of carbons of the fused ring with thiophene hamper the hydrogen bond between the carbonitrile fragment with asparagine 152 (Figure 7C). Even the conformations of **ACS_{05}** and **ACS_{06}** aren't the same, but show the same hydrogen bond interactions of ether oxygen with residues asparagine 143, threonine 148, valine 149 and, carbonyl oxygen with serine 150 and asparagine 152. These results indicated that pyruvate kinase enzyme can be a putative target of the thiophene-acridine

derivatives synthesized in this work. Future analysis will be performed to better elucidate the mechanism of action against leishmaniasis.

4. Conclusion

Eight new thiophene-acridine compounds were designed, synthesized with good efficiency and well characterized by physicochemical and spectral data (^{1}H and ^{13}C NMR, IR and HRMS). These compounds were investigated for their cytotoxic and antileishmanial properties against promastigote forms of *L. (L.) amazonensis*. It was observed that the evaluated substances, whose IC_{50} values were lower than 10 µM, presented better activity than the reference drugs (tri and pentavalent antimony). The most active compounds were **ACS_{01}** and **ACS_{02}**, with IC_{50} of 9.60±3.19 and 10.95±3.96 µM, respectively. On the highest concentration tested, none of the compounds tested presented cytotoxicity for human erythrocytes, demonstrating that all compounds evaluated are less toxic for blood cells than the reference drugs. The thiophene-acridine derivatives were more selective for the parasite than for blood cells, with selectivity index better than those for reference drugs. The derivatives **ACS_{01}** and **ACS_{02}** were efficient against parasites resistant to the trivalent antimony. The activity antileishmanial of **ACS_{01}** was not associated to DNA fragmentation. However, the compounds **ACS_{01}** and **ACS_{02}** presented *in vitro* DNA Kb of 10^4 M^{-1}, characteristic of DNA intercalating agents. There was a correlation between the lipophilicity of the molecules and antileishmanial activity highlighted by the PLS data. Molecular docking findings demonstrated correlation between the values of pIC_{50} and inhibition of pyruvate kinase enzyme, where the presence of ring thiophene, especially with ester and nitrile functions were important for interaction with the target. In addition, the methoxy-acridine nucleus was able to intercalate into the DNA and also interacted with the enzyme pyruvate kinase through its methoxyl, which indicates the duality of mechanism of action of the new derivatives. Based on the results, it can be suggested that the thiophene-acridine compounds can be considered promising for the development of new drugs for the treatment of leishmaniasis.

Acknowledgements

We would like to extend our gratitude to our supporters and partners; UFPB, UFPE, UEPB and CAPES for the financial and structural support for this study.

Supplementary data

Supplementary data associated with this article can be found in the online version.

Figure Legends

Scheme 1. Synthesis of 2-amino-thiophene and the new hybrid thiophene-acridine compounds. Reagents and conditions: (a) morpholine, sulfur, EtOH, 5 - 10°C, 3h; (b) 9-acrinaldehyde (**AC_{02}**), EtOH, 60ºC, 5h. (c) 6,9-dichloro-2-methoxy-acridine (**ACS**), EtOH, AcOH, rt, 4h.

Figure 1. (A) Absorption spectra of ACS_{01} and ACS_{02} (30 µM) with increasing concentrations of ctDNA. [DNA] = 0 (black), 10 (red), 20 (green), 40 (yellow), 60 (blue), 80 (pink) and 100 (light blue) µM. Arrow (↑) refers to hyperchromic effect. (B) The plot of $[DNA]/(\varepsilon_a - \varepsilon_f)$ as function of DNA concentration as determined from the absorption spectral data.

Figure 2. Fluorescence spectra of ACS_{01} (A) and ACS_{02} (B) (10 µM) with increasing concentrations of ctDNA. [DNA] = 0 (black), 10 (red), 20 (green), 40 (yellow), 60 (blue), 80 (pink) and 100 (light blue) µM. Arrow (↓) refers to hypochromic effect.

Figure 3. (A) Plot of r2 and q2 versus the number of latent variables (LV) used in PLS models. (B) Plot of experimental versus recomputed values of pIC_{50} generated with the PLS model by using 2 latent variables and 15 descriptors for 16 structures. (C) Plot of experimental versus predicted values of pIC_{50} values by leave-one-out cross-validation method.

Figure 4. (A) Coefficients plot generated from the selected PLS model. (B) Loadings plot generated from the selected PLS model.

Figure 5. Scores plot of the selected PLS mode (see table 2 in supporting data).

Figure 6. (A) Hydrophobic (green) and hydrophilic (blue) regions of compounds 6AMD (pIC_{50} = 3.37) and ACS_{01} (pIC_{50} = 5.01) generated at -1.0 kcal/mol and -3.0kcal/mol

respectively. (B) Hydrophobic (green) regions of compounds 6AMD (pIC50 = 3.37) and AC_{02} (pIC50 = 4.97) generated at -0.2 kcal/mol.

Figure 7. (A) Interactions between the active site of pyruvate kinase of *L. mexicana* and ligand ABH and compound ACS_{01}. (B) Interactions between the active site of pyruvate kinase of *L. mexicana* and ligands ACS_{01} to ACS_{04}. The distance between carbonitrile and asparagine 152 increases with the number of carbons of the fused ring of thiophene. (C) Interactions between the active site of pyruvate kinase of *L. mexicana* and ligands ACS_{05} and ACS_{06}.

Figure Legends for Supporting Information

Figure 1. NMR ^{1}H of compound ACS_{01}

Figure 2. NMR ^{13}C of compound ACS_{01}

Figure 3. IR of compound ACS_{01}

Figure 4. HRMS of compound ACS_{01}

Figure 5. NMR ^{1}H of compound ACS_{02}

Figure 6. NMR ^{13}C of compound ACS_{02}

Figure 7. IR of compound ACS_{02}

Figure 8. HRMS of compound ACS_{02}

Figure 9. NMR ^{1}H of compound ACS_{03}

Figure 10. NMR ^{13}C of compound ACS_{03}

Figure 11. IR of compound ACS_{03}

Figure 12. HRMS of compound ACS_{03}

Figure 13. NMR ^{1}H of compound ACS_{04}

Figure 14. IR of compound ACS_{04}

Figure 15. HRMS of compound ACS_{04}

Figure 16. NMR ^{1}H of compound ACS_{05}

Figure 17. NMR ^{13}C of compound ACS_{05}

Figure 18. IR of compound ACS_{05}

Figure 19. HRMS of compound ACS_{05}

Figure 20. NMR ^{1}H of compound ACS_{06}

Figure 21. NMR ^{13}C of compound ACS_{06}

Figure 22. IR of compound ACS_{06}

Figure 23. HRMS of compound ACS_{06}

Figure 24. NMR ^{1}H of compound ACS_{07}

Figure 25. NMR ^{13}C of compound ACS_{07}

Figure 26. IR of compound ACS_{07}

Figure 27. HRMS of compound ACS_{07}

Figure 28 (Graph S1). Growth inhibition of the promastigote forms of *Leishmania (L.) amazonensis* in presence of different concentrations of moieties 2-amino-tiophen and 6,9-diclhoro-2-methoxi-acridine.

Figure 29 (Graph S2). Growth inhibition of the promastigote forms of *Leishmania amazonensis* in presence of different concentrations of hybrids derivatives thiophene-acridine serial ACS.

Figure 30 (Graph S3). Growth inhibition of the promastigote forms of *Leishmania (L.) amazonensis* in presence of different concentrations of the reference drugs: Glucantime®, Trivalent antimonial and Amphotericin B.

Conflict of Interest

The authors declare that there was no competing interests.

References

[1] A. Cavalli, M.L. Bolognesi, Neglected tropical diseases: multi-target-directed ligands in the search for novel lead candidates against Trypanosoma and Leishmania, J. Med. Chem. 52 (2009) 7339-7359.

[2] WORLD HEALTH ORGANIZATION (WHO), 2015. Diseases covered by NTD Department. <http://www.who.int/neglected_diseases/diseases/en/>. (Acessed in 12 mar 2016).

[3] P.L.N. Néris, J.P.A. Caldas, Y.K.S. Rodrigues, F.M. Amorim, J.A. Leite, S. Rodrigues-Mascarenhas, J.M. Barbosa-Filho, L.C. Rodrigues, M.R. Oliveira, Neolignan Licarin A presents effect against Leishmania (Leishmania) major associated with immunomodulation in vitro, Exp. Parasitol. 135 (2013) 307-313.

[4] S. Mohapatra, Drug resistance in leishmaniasis: Newer developments, Trop. Parasitol. 4 (2014) 4-9.

[5] C. Viegas-Júnior, A. Danuello, V.S. Bolzani, E.J. Barreiro, C.A.M. Fraga, Molecular hybridization: a useful tool in the design of new drug prototypes, Curr. Med. Chem. 14 (2007) 1829-1852.

[6] S.M. Almeida, E.A. Lafayette, W.L. Silva, V.L. Serafim, T.M. Menezes, J.L. Neves, A.L. Ruiz, J.E. Carvalho, R.O. Moura, E.I. Beltrão, L.B. Carvalho-Júnior, M.D. Lima, New spiro-acridines: DNA interaction, antiproliferative activity and inhibition of human DNA topoisomerases. Int J Biol Macromol. 92 (2016) 467-475.

[7] F.W.A. Barros, T.G. Silva, M.G.R. Pitta, D.P Bezerra, L.V. Costa-Lotufo, M.O. Moraes, C. Pessoa, M.A.F.B. Moura, F.C. Abreu, M.C.A. Lima, S.L. Galdino, I.R. Pitta, M.O.F. Goulart, Synthesis and cytotoxic activity of new acridine-thiazolidine derivatives, Bioorg. Med. Chem. 20 (2012) 3533-3539.

[8] B.B. Patel, R.G. Patel, M.P. Patel, Synthesis and studies of the biological activity of novel pyrimidino fused acridine derivatives, J. Serb. Chem. Soc. 71 (2006) 1015-1023.

[9] S.M. Sondhi, J. Singh, R. Rani, P.P. Gupta, S.K. Agrawal, A.K. Saxena, Synthesis, anti-inflammatory and anticancer activity evaluation of some novel acridine derivatives, Eur. J. Med. Chem. 45 (2010) 555-563.

[10] V. Tomar, G. Bhattacharjee, S. Rajakumar, K. Srivastava, S.K. Puri, Synthesis of new chalcone derivatives containing acridinyl moiety with potential antimalarial activity, Eur. J. Med. Chem. 45 (2010) 745-751.

[11] L. Fang, D. Appenroth, M. Decker, M. Kiehntopf, C. Roegler, T. Deufel, C. Fleck, S. Peng, Y. Zhang, J. Lehmann, Synthesis and biological evaluation of NO-donor-tacrine hybrids as hepatoprotective anti-Alzheimer drug candidates, J. Med. Chem. 51 (2008) 713-716.

[12] S.A. Gamage, D.P. Figgitt, S.J. Wojcik, R.K. Ralph, A. Ransijn, J. Mauel, V. Yardley, D. Snowdon, S.L. Croft, W.A. Denny, Structure-activity relationships for the antileishmanial and antitrypanosomal activities of 1'-substituted 9-anilinoacridines, J. Med. Chem. 40 (1997) 2634-2642.

[13] C. Gao, F. Liu, X. Luan, C. Tan, H. Liu, Y. Xie, Y. Jin, Y. Jiang, Novel synthetic 2-amino-10-(3,5-dimethoxy)benzyl-9(10H)-acridinone derivatives as potent DNA-binding antiproliferative agentes, Bioorg. Med. Chem. 18 (2010) 7507-7514.

[14] E.A. Lafayette, S.M.V. Almeida, M.G.R. Pitta, E.I.C. Beltrão, T.G. Silva, R.O. Moura, I.R. Pitta, L.B. Carvalho Júnior, M.C.A. Lima, Synthesis, DNA binding and topoisomerase I inhibition activity of thiazacridine and imidazacridine derivatives, Molecules, 18 (2013) 15035-15050.

[15] L. Janovec, M. Kozurková, D. Sabolová, J. Ungvarský, H. Paulíková, J. Plsíková, Z. Vantosá, J. Imrich, Cytotoxic 3,6-bis((imidazolidinone)imino)acridines: synthesis, DNA binding and molecular modeling, Bioorg. Med. Chem. 19 (2011) 1790-1801.

[16] Q. Liu, J. Zhang, M.Q. Wang, D.W. Zhang, Q.S. Lu, Y. Huang, H.H. Lin, X.Q. Yu, Synthesis, DNA binding and cleavage activity of macrocyclic polyamines bearing mono- or bis-acridine moieties, Eur. J. Med. Chem. 45 (2010) 5302-5308.

[17] S.M.V. Almeida, E.A. Lafayette, L.P.B.G. Silva, C.A.C. Amorim, T.B. Oliveira, A.L.T.G. Ruiz, J.E. Carvalho, R.O. Moura, E.I.C. Beltrão, M.C.A. Lima, L.B. Carvalho-Júnior, Synthesis, DNA Binding, and Antiproliferative Activity of Novel Acridine-Thiosemicarbazone Derivatives, Int. J. Mol. Sci. 16 (2015) 13023-13042.

[18] C. Di Giorgio, K. Shimi, G. Boyer, F. Delmas, J.P. Galy, Synthesis and antileishmanial activity of 6-mono-substituted and 3,6-di-substituted acridines obtained by acylation of proflavine, Eur. J. Med. Chem. 42 (2007) 1277-1284.

[19] I.L.K. Wong, K.F. Chan, Y. Zhao, T.H. Chan, L.M. Chow, Quinacrine and a novel apigenin dimer can synergistically increase the pentamidine susceptibility of the protozoan parasite Leishmania, J. Antimicrob. Chemother. 63 (2009) 1179-1190.

[20] K.A.F. Rodrigues, C.N.S. Dias, P.L.N. Néris, J.C. Rocha, M.T. Scotti, L. Scotti, S.R. Mascarenhas, R.C. Veras, I.A. Medeiros, T.S.L. Keesena, T.B. Oliveira, M.C.A. Lima, T.L. Balliano, T.M. Aquino, R.O. Moura, F.J.B. Mendonça-Junior, M.R. Oliveira, 2-Amino-thiophene derivatives present antileishmanial activity mediated by apoptosis and immunomodulation *in vitro*, Eur. J. Med. Chem. 106 (2015) 1-14.

[21] M.B. Félix, E.R. Souza, M.C.A Lima, D.K.G. Frade, V.L. Serafim, K.A.F. Rodrigues, P.L.N. Néris, F.F. Ribeiro, L. Scotti, M.T. Scotti, T.M. Aquino, F.J.B. Mendonça-Junior, M.R. Oliveira, Antileishmanial activity of new thiophene-indole hybrids: Design, synthesis, biological and cytotoxic evaluation, and chemometric studies, Bioorg. Med. Chem. 24 (2016) 3972-3977.

[22] L.A. Fothergill-Gillmore, D.J. Rigden, P.A. Michels, S.E Phillips, The structure of pyruvate kinase from Leishmania mexicana reveals details of the allosteric transition and unusual effector specificity. J Mol Biol 291 (1999) 615–635.

[23] V. Hannaert, C. Yernaux, D.J. Rigden, L.A. Fothergill-Gilmore, F.R. Opperdoes, P.A. Michels, The putative effector-binding site of *Leishmania Mexicana* pyruvate kinase studied by site-directed mutagenesis. FEBS Lett 514 (2002) 255–259

[24] Bakker B.M., Michels P.A.M, Opperdoes F.R., Westerhoff H.V., Glycolysis in bloodstream form *Trypanosoma brucei* can be understood in terms of the kinetics of the glycolytic enzymes. J. Biol. Chem. 272 (1997) 3207-3215.

[25] F.J.B. Mendonça-Junior, R.G. Lima-Neto, T.B. Oliveira, M.C.A. Lima, I.R. Pitta, S.L. Galdino, R.M.D. Cruz, R.S.A. Araújo, R.P. Neves, Synthesis and evaluation of the antifungal activity of 2-(substituted-amino)-4,5-dialkyl-thiophene-3-carbonitrile derivatives, Lat. Am. J. Pharm. 30 (2011) 1492-1499.

[26] B.C.C. Souza, T.B. Oliveira, T.M. Aquino, M.C.A. Lima, I.R. Pitta, S.L. Galdino, M.T. Scotti, E.O. Lima, T.G. Silva, G.C. Militão, L. Scotti, F.J.B. Mendonça-Junior, Preliminary antifungal and cytotoxic evaluation of synthetic cycloalkyl[b]thiophene derivatives with PLS-DA analysis, Acta Pharm. 62 (2012) 221-236.

[27] A. Wolfe, G.H. Shimer, T. Meehan, Polycyclic aromatic hydrocarbons physically intercalate into duplex regions of denatured DNA, Biochemistry. 26 (1987) 6392-6396.

[28] J.D. McGhee, P.H. Von Hippel, Theoretical aspects of DNA-protein interactions: co-operative and non-co-operative binding of large ligands to a one-dimensional homogeneous lattice, J. Mol. Biol. 86 (1974) 469-489.

[29] G. Cruciani, M. Pastor, R. Mannhold, Suitability of molecular descriptors for database mining. A comparative analysis, J. Med. Chem. 45 (2002) 2685-2694.

[30] L. Scotti, E.I. Ferreira, M.S. Silva, M.T. Scotti, Chemometric studies on natural products as potential inhibitors of the NADH oxidase from *Trypanosoma cruzi* using the VolSurf approach, Molecules. 15 (2010) 7363-7377.

[31] I.R.A. Menezes, J.C.D. Lopes, C.A. Montanari, G. Oliva, F. Pavao, M.S. Castilho, P.C. Vieira, M.T. Pupo, 3D QSAR studies on binding affinities of coumarin natural products for glycosomal GAPDH of *Trypanosoma cruzi*, J. Comput. Aid. Mol. Des. 17 (2003) 277-290.

[32] P. Geladi, B.R. Kowalski, Partial least-squares regression: a tutorial, Anal. Chim. Acta. 185 (1986) 1-17.

[33] F. Real, R.O. Vidal, M.F. Carazzolle, J.M.C. Mondego, G.G.L. Costa, R.H. Herai, M. Würtele, L.M. Carvalho, R.C. Ferreira, R.A. Mortara, C.L. Barbiéri, P. Mieczkowski, J.F. Silveira, M.R.S. Briones, G.A.G. Pereira, D. Bahia, The genome sequence of *Leishmania* (*Leishmania*) *amazonensis*: functional annotation and extended analysis of gene models, DNA Res. 20 (2013) 567-581.

[34] H.P. Morgan, I.W. McNae, M.W. Nowicki, W. Zhong, P.A. Michels, D.S. Auld, L.A. Fothergill-Gilmore, M.D. Walkinshaw, The trypanocidal drug suramin and other trypan blue mimetics are inhibitors of pyruvate kinases and bind to the adenosine site, J. Biol. Chem. 286 (2011) 31232-31240.

[35] R. Thomsen, M.H. Christensen, MolDock: a new technique for high-accuracy molecular docking, J. Med Chem. 49 (2006) 3315-3321.

[36] E.L. D'Antonio, B. Ullman, S.C. Roberts, U.G. Dixit, M.E. Wilson, Y. Hai, D.W. Christianson, Crystal structure of arginase from *Leishmania mexicana* and implications for the inhibition of polyamine biosynthesis in parasitic infections, Arch. Biochem. Biophys. 535 (2013) 163-176.

[37] C.M.R. Ribeiro, N.A. Souza, General scheme for elucidating the structure of organic compounds using spectroscopic and spectrometric methods, Quím. Nova. 30 (2007) 1026-1031.

[38] D. Plano, Y. Baquedano, D. Moreno-Mateos, M. Font, A. Jiménez-Ruiz, J.A. Palop, C. Sanmartín, Selenocyanates and diselenides: a new class of potent antileishmanial agents, Eur. J. Med. Chem. 46 (2011) 3315-3326.

[39] R. P. McGeary, D. T.C. Tan, C. Selleck, M. M. Pedroso, H. E. Sidjabat, G. Schenk. Structure-activity relationship study and optimisation of 2-aminopyrrole-1-benzyl-4,5-diphenyl-1H-pyrrole-3-carbonitrile as a broad spectrum metallo-β-lactamase inhibitor. Eur. J. Med. Chem. 137 (2017) 351-364.

[40] N. Busto, B. Garcia, J.M. Leal, F. Secco, M. Venturini, The mode of binding ACMA-DNA relies on the base-pair nature, Org. Biomol. Chem. 10 (2012) 2594-2602.

[41] H. Ihmels, D. Otto, Intercalation of organic dye molecules into double-stranded DNA general principles and recent developments Top. Curr. Chem. 258 (2005) 161-204.

[42] W. Zhang, B. Zhang, W. Zhang, T. Yang, N. Wang, C. Gao, C. Tan, H. Liu, Y. Jiang. Synthesis and antiproliferative activity of 9-benzylamino-6-chloro-2-methoxy-acridine derivatives as potent DNA-binding ligands and topoisomerase II inhibitors. Eur. J. Med. Chem. 116 (2016) 59-70.

[43] S.M.V. Almeida, L.P.B. Silva, L.R. Lima, G.B. Longato, R.J. Padilha, L.C. Alves, F.A. Brayner, A.L. Ruiz, J.E. Carvalho, E.I.C. Beltrão, M.C.A. Lima, L.B. Carvalho-Jr, Ultrastructural Assessment of 2-(acridin-9-ylmethylene)-N-

phenylhydrazinecarbothioamideactivity on human breast adenocarcinoma cells, Micron 90 (2016) 114-122.

[44] S. Bongarzone, M. L. Bolognesi, The concept of privileged structures in rational drug design: focus on acridine and quinoline scaffolds in neurodegenerative and protozoan diseases. Expert Opin Drug Discov 6 (2011) 251-268.

[45] S. Jamal, V. Scaria, Cheminformatic models based on machine learning for pyruvate kinase inhibitors of *Leishmania Mexicana*, BMC Bioinform. 14 (2013) 1-7.

[46] R. Ochoa, S.J. Watowich, A. Florez, C.V. Mesa, S.M. Robledo, C. Muskus, Drug search for leishmaniasis: a virtual screening approach by grid computing, J. Comput. Aided. Mol. Des. 30 (2016) 541-552.

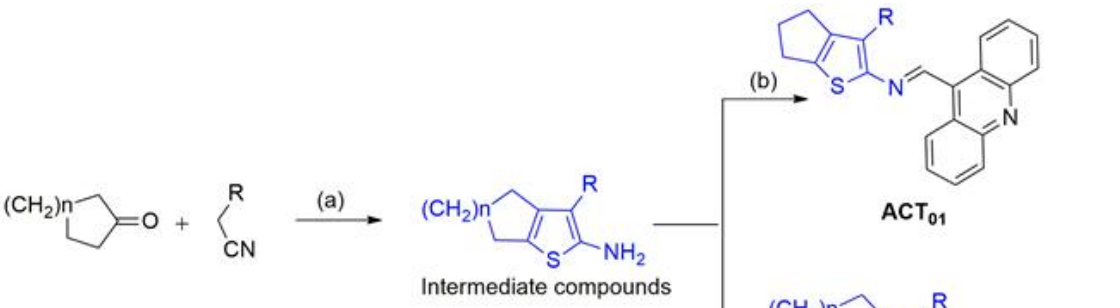

Intermediate compound	Final compound	$(CH_2)n$	R
5CN	ACS_{01}	1	-CN
6CN	ACS_{02}	2	-CN
7CN	ACS_{03}	3	-CN
8CN	ACS_{04}	4	-CN
6EST	ACS_{05}	1	$CO_2C_2H_5$
7EST	ACS_{06}	2	$CO_2C_2H_5$
6AMD	ACS_{07}	1	$CONH_2$

Table 1. Data on 50% growth inhibition of the parasite population (IC_{50}±SEM), cellular viability (HC_{50}) and selectivity index (SI).

Compounds	**n**	**R**	**IC_{50} (μM)**	**HC_{50} (μM)**	**SI**
ACS	-	-	229.46±10.78	>1000	>4.35
AC02	-	-	10.66±4.31	>1000	>93.80
5CN	1	-C≡N	87.68±4.00	>1000	>11.40
6CN	2	-C≡N	181.76±5.46	>1000	>5.50
7CN	3	-C≡N	94.28±11.78	>1000	>10.60
8CN	4	-C≡N	66.40±8.91	>1000	>15.06
6EST	2	$CO_2C_2H_5$	83.62±7.72	>1000	>11.95
7EST	3	$CO_2C_2H_5$	88.87±12.97	>1000	>11.25
6AMD	2	$CONH_2$	429.02±18.67	>1000	>2.33
ACT_{01}	1	-C≡N	>500	ND	NE
ACS_{01}	1	-C≡N	9.60±3.19	>1000	>104.16
ACS_{02}	2	-C≡N	10.95±3.96	>1000	>91.32
ACS_{03}	3	-C≡N	32.26±5.50	>1000	>30.99
ACS_{04}	4	-C≡N	68.97±4.85	>1000	>14.49
ACS_{05}	2	$CO_2C_2H_5$	26.55±3.98	>1000	>37.66
ACS_{06}	3	$CO_2C_2H_5$	31.80±5.86	>1000	>31.44
ACS_{07}	2	$CONH_2$	51.37±13.14	>1000	>19.46
Glucantime	-	-	>1000	>1000	>1
Trivalent Antimony	-	-	14.77±0.52	565.62±68.99	38.29
Amphotericin B	-	-	0.19±0.09	24.25±2.52	127.63

ND – not determined; NE – not estimated

Table 2. Antileishmanial activity of thiophene-acridine compound **ACS_{01}** and **ACS_{02}** on promastigote forms of *L*. (L.) *amazonensis*, both sensitive and resistant to the trivalent antimony.

	IC_{50} (±SEM)	
Compound	Sensitive strain	Resistant strain
ACS_{01}	14.04±1.46	14.83±0.44
ACS_{02}	16.05±1.38	16.36±1.72

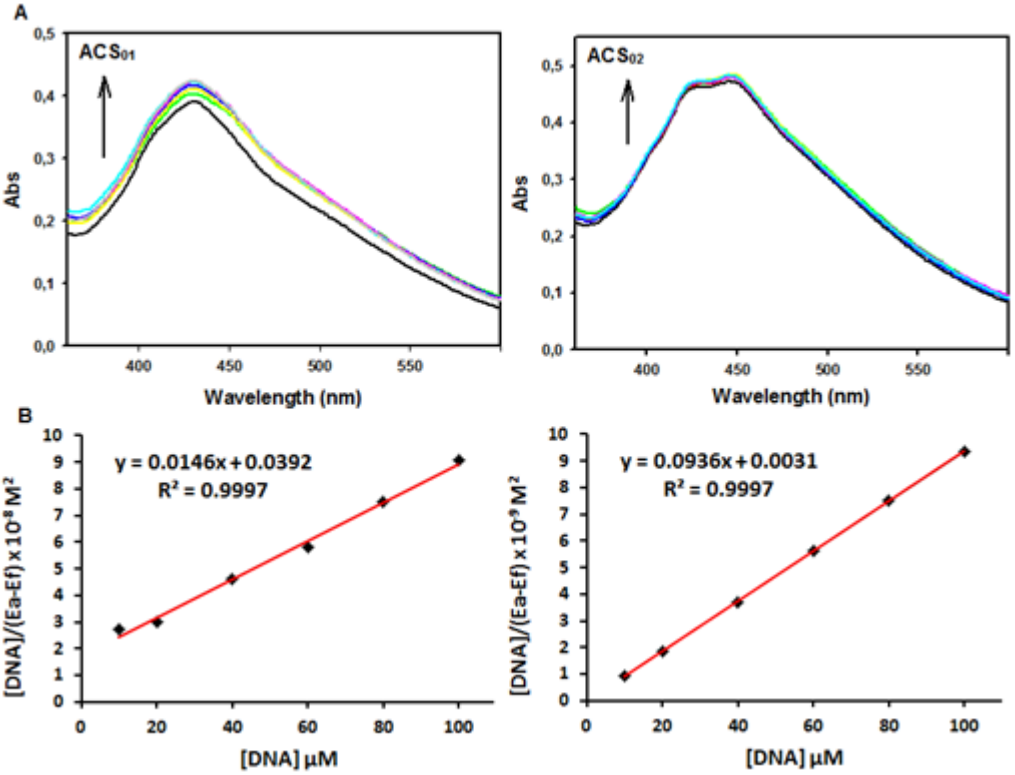

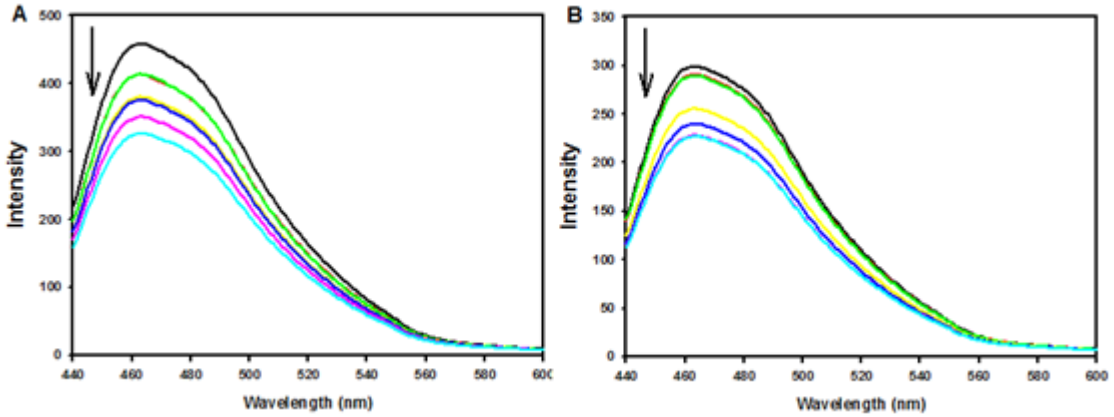

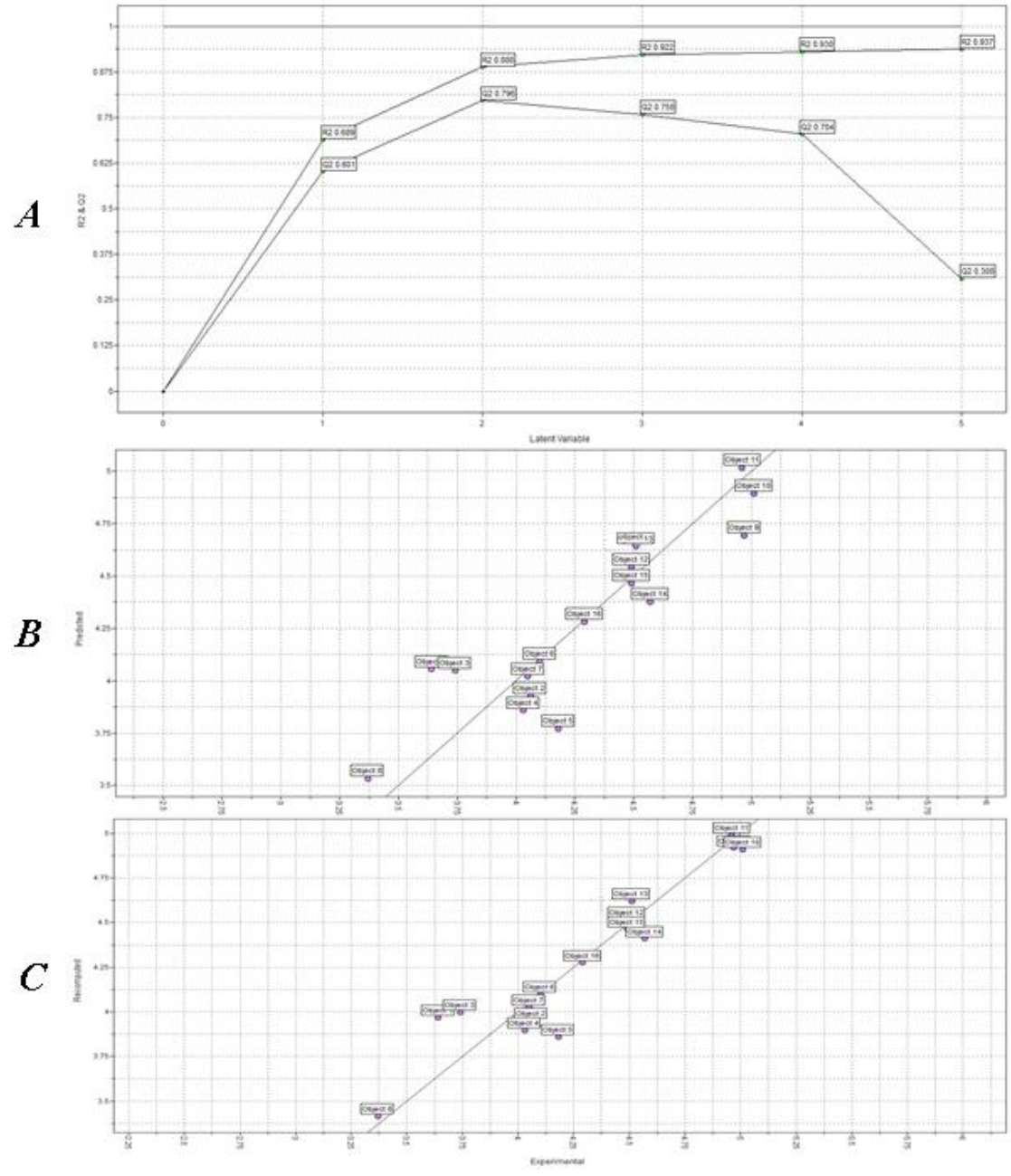

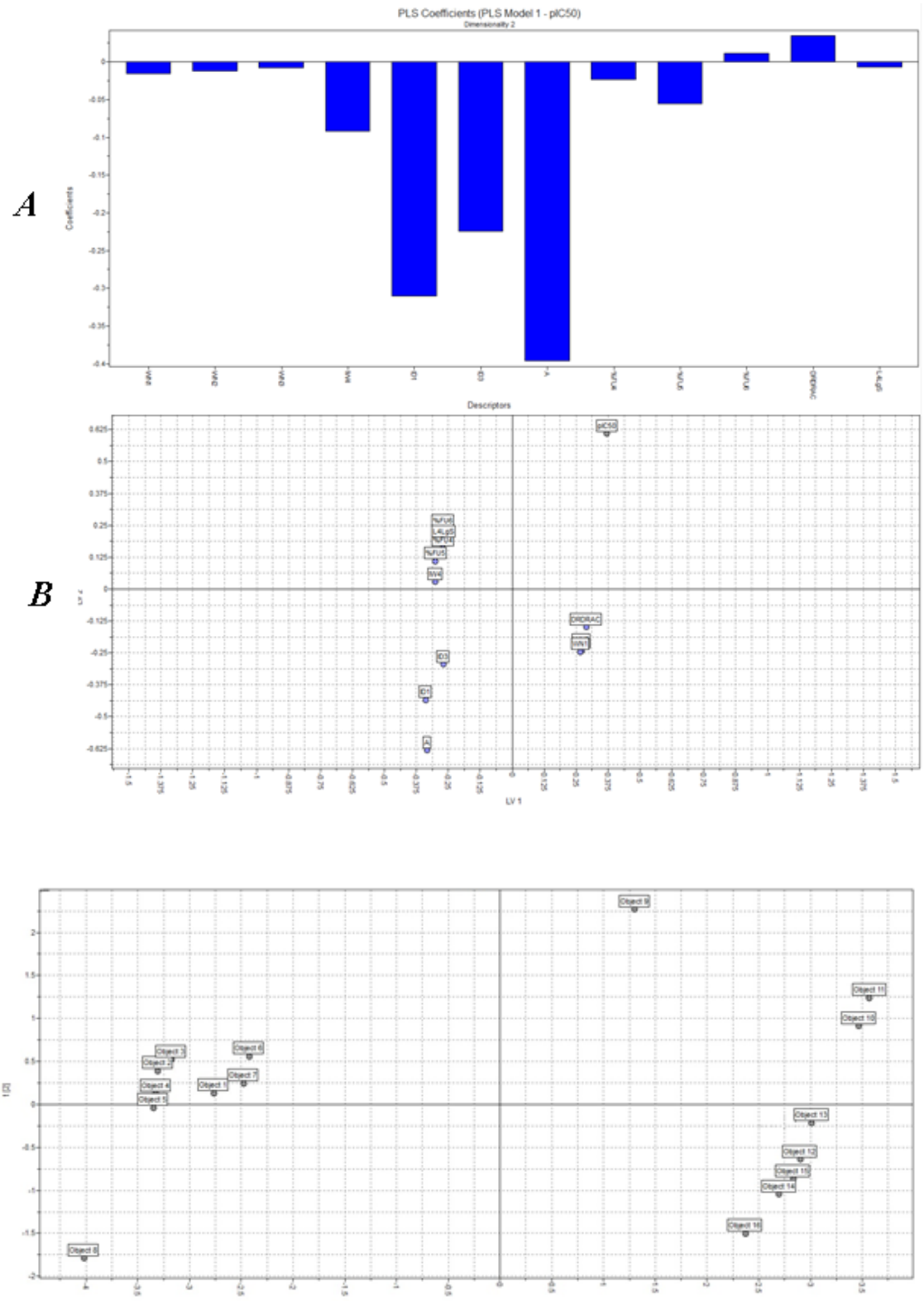

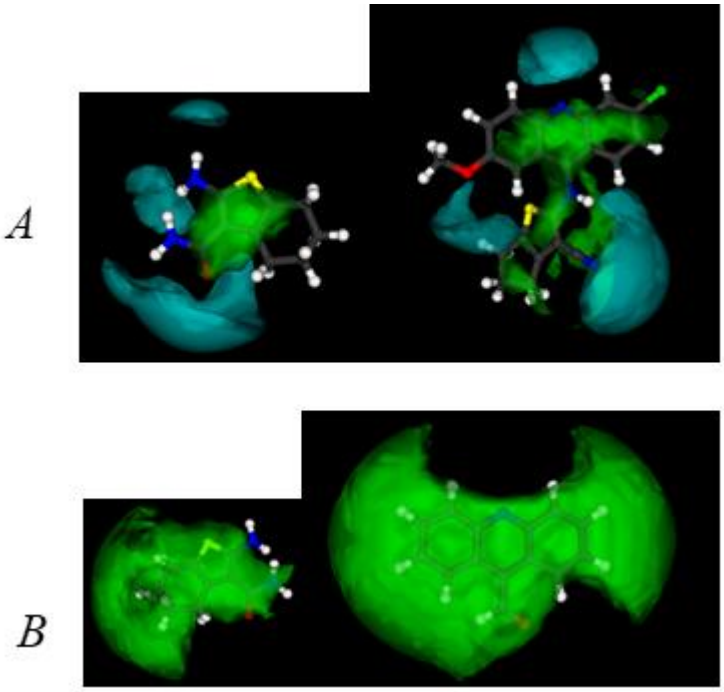

A

B

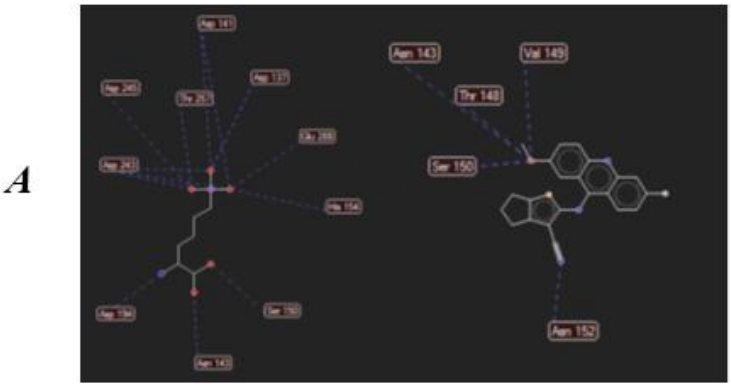

A

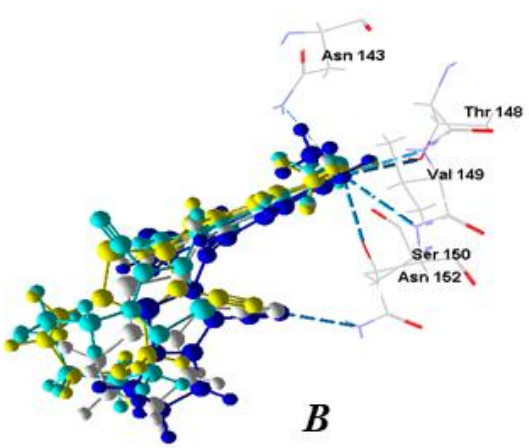

B

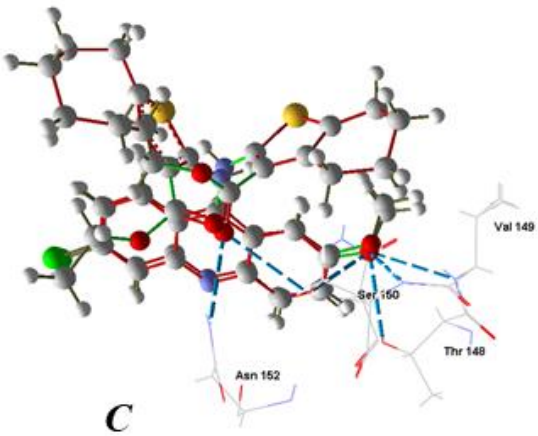

C